



INTERNATIONAL JOURNAL OF TRENDS IN EMERGING RESEARCH AND DEVELOPMENT

INTERNATIONAL JOURNAL OF TRENDS IN EMERGING RESEARCH AND DEVELOPMENT

Volume 1; Issue 1; 2023; Page No. 403-407

Received: 16-08-2023

Accepted: 29-10-2023

To assess the quality of our model of choice, to multiple instances learning setting in CT scans

¹Sunil Appaso Kumbhar and ²Dr. Amit Singhal

¹Research Scholar, Monad University, Hapur, Uttar Pradesh, India

²Professor, Monad University, Hapur, Uttar Pradesh, India

Corresponding Author: Sunil Appaso Kumbhar

Abstract

A human body has 206 individual bones. The skeleton of an organism is composed of bone, a hard substance. The honeycomb-like matrix that provides tension to bones is an interior component of the connective tissue bone, which is composed of several cell types. Building the framework for the body and facilitating movement are the main roles of bones. Cancer of the bone may develop in any bone in the body. U.S. cancer statistics for 2023 are out from the American Cancer Society (ACS). These are the key takeaways: The anticipated number of cancer-related fatalities in 2023 is 609,820 (or about 1,670 per day), with roughly 1.9 million new cases (or about 5,370 per day) of cancer overall. Bone tumours may be either benign or cancerous. Both primary bone tumours and tumours that metastasize to the skeleton may develop in the body. Based on their initial site of development, bone tumours are categorized as either primary or secondary. The third There are a variety of approaches that physicians might use in order to identify bone cancer. Bone biopsies, X-rays, PET, CT, and MRI are all part of this category. There are benefits and drawbacks to each of these approaches; ultimately, physicians will select the one that works best for their individual patients.

Keywords: Skeleton, Bones, Computed Tomography, Biopsies, Cancer

1. Introduction

In comparison to the neural network, the hidden layer—an intermediate layer—has more layers. An individual neurone is the building block of a network. Deep learning differs from device learning in that it moves in the direction of its objective, whereas device learning is perpendicular. The breast cancer dataset is categorized using a Convolution Neural Network. The pictures are sorted using a convolutional Neural Network. It reads the bone cancer dataset's pictures as input. Convolutional neural networks (CNNs) accept the pictures and their weights as input. A reduction in mistake and an improvement in performance are the goals of the weight adjustments. Pooling, ReLU, fully connected, and many more layers make up convolutional neural networks (CNNs), and convolutional. There are many layers in a convolutional neural network (CNN), the most common of which are the pooling, ReLU, fully connected, and convolutional layers. A characteristic map is used by the convolution layer to decrease the input picture's size while simultaneously extracting its functions. Reducing the image's dimensions is done using the pooling

layer As an activation function, the ReLU layer checks whether the value of the activation function is within a certain range. The model culminates with the totally linked layer.

For men and women alike, cancer ranks as the top killer. Cancer has emerged as the leading health and medical concern of our day. By using image processing as a conclusive technique, doctors could be useful for detecting cancer at an early stage, which is crucial for improving and extending survival rates. Uncontrolled cell proliferation in the bone, a disease known as bone cancer occurs. By detecting cancer early on, a complete cure is within reach. Currently, there is a lot of prioritise the development of tools for the early diagnosis of cancerous nodules. The process of cancer spreading from its original site in the bone to other organs and tissues is called metastasis. Early detection of uncontrolled development allows for a range of therapeutic options, decreasing the likelihood of needless surgery and improving the likelihood of survival.

Radiation therapy, chemotherapy, and surgery are further therapeutic choices. There are a lot of variables that affect

survival rates. Although several variables come into play, including the patient's overall health, just 14% of those diagnosed with bone cancer manage to live five years after the diagnosis. Often, the symptoms aren't obvious, making it hard to know what stage of disease you're in. Radiology, CT scans, magnetic resonance imaging (MRI), and x-rays are the three most used methods for imaging bones. On an X-ray, a possible sarcoma looks like a hole in the bone. In x-rays, which are high-energy electromagnetic radiations, the body is shown in greyscale. CT scans provide cross-sectional pictures of the body by using technology that is analogous to X-rays. One such method is MRI, or magnetic resonance imaging, which takes use of radio waves and strong magnets to provide a detailed image of a targeted organ or tissue. Images produced by imaging modalities such as X-ray and CT are more accurate and detailed. Because of this, hybrid imaging modalities are gaining popularity; they include the greatest aspects of several approaches while compensating for their limitations.

2. Review of Literature

Abhilasha Shukla *et al.* (2020) Discuss the characteristics of bone cancer and how they may be used to determine the kind of cancer in this article. Related work that using computer vision to identify human cancer is covered in this publication. You may segment x-ray and MRI pictures using the methods outlined in this study, including Sobel, Prewitt, Canny, and Region Growing Image Segmentation. Also included in the publication are the outcomes of MATLAB-based bone osteosarcoma cancer detection utilizing X-ray image segmentation using edge-based and area-based methods. Finding the optimal segmentation method for a greyscale image with possible consequences was the last step in the paper's conclusion. It seems that the best methods for finding cancer bone from X-Ray pictures are k-mean and region-growing image segmentation.

Terapap Apiparakoon *et al.* (2020) showcase an innovative method for segmenting and categorizing atypical hotspots; this approach is a semi-supervised method for treating chest metastases from bone cancer. The model that has been suggested, MaligNet, is an instance segmentation model that collects both labelled and unclassified data using ladder grids. A dataset is required to evaluate the proposed model's performance will be generated using both labelled and unlabeled data from 544 and 9280. With mean scores of 0.852 for accuracy, 0.856 for sensitivity, and 0.848 for F1score, the suggested model outperformed a CNN trained on the core mask region, the Mask-R, CNN, by 3.92%. There is promising future for automated diagnostics employing bone scintigraphy in clinical practice, as 0.657 for sensitivity and 0.857 for specificity are the results that the model achieves in the metastatic classification mission.

Eftekhari Hossain (2018) introduced one way to use neurofuzzy classifier and fuzzy clustering to identify and categorise bone cancer. We want to find out if bone cancer may be detected using a fuzzy C-mean clustering algorithm. One hundred twenty-two MRI scans of the bone were used to ensure the suggested technique was accurate. Inference System (ANFIS) to distinguish between noncancerous and cancerous bone cancers. The ANFIS network was trained and tested using GLCM extracted from MR images. The bone pictures that were correctly undergone cross-validation

when used for testing and training. Three output matrices were used to assess the classification result's accuracy, sensitivity, and specificity. An accuracy percentage of 93.75% was achieved by the suggested strategy for classifying bone cancer.

3. Objectives of the study

1. To study in Bone structure labeling in CT scans
2. To assess the quality of our model of choice, to multiple instances learning setting.

4. Research Methodology

The viewing experience may be improved with the use of more sophisticated display systems. For an X-ray-like picture, make use of average intensity projections or maximum intensity projections, which combine information from several slices simultaneously.

A more involved approach is to use direct volume rendering methods, including ray casting. These projections are still two-dimensional, but they make it possible to get results that appear three-dimensional. For a demonstration of ray casting with two distinct transfer functions, bottom row. Based on the scientific principles of emission, absorption, and scattering, ray casting creates a two-dimensional picture by simulating the path of a light beam passing through a solid object. The next step is to sample the volume at equidistant positions along each of these beams. It is necessary to interpolate in order to place these sample points between voxels. Every sample point's colour, lightness, and transparency values are calculated with the use of a transfer function. If we wanted to highlight bones in CT using a simple transfer function, for instance, we could use full transparency everywhere else and white with complete opacity to represent HU values inside the bone range. Finally, like using a sheet of foil projected onto a ceiling-mounted screen, the values of the sample points along a ray are mixed to give the present pixel its colour value.

The majority of systems use early ray termination to expedite the process. After then, the sample points are only taken into account until the opacity channel is almost filled. Further calculations would have no effect on the end outcome since everything beyond this point is concealed by opaque materials.

Although the ability to observe a certain kind of tissue is made possible via a transfer function, it is unable to distinguish between multiple instances of that tissue, for example, distinguishing individual bones.

5. Results and data interpretation: Getting a big enough training set of annotated data might be a real challenge when using deep learning methods for a segmentation problem. Even when done by professionals, labelling is a laborious operation whose outcomes the operator's expertise plays a crucial role. The ground-truth pictures were obtained in this study by applying a variety of processes on the original scans. This was achieved by using MeVisLab, a research platform MeVis Medical Solutions Ag collaborated with Fraunhofer MEVIS, a research organisation, to develop a semi-automatic preprocessing network for use in image processing. This system was used to preprocess the original scans, and then each slice was manually examined to fix the problems that were found often.

5.1 MeVisLab network

Extraction of just an abdominal computed tomography scan's skeleton is achieved by a series of thresholding and image processing processes implemented on the MeVisLab network. While the last ground truth is shown on the right, three axial sections of abdomen CT scans are presented on the left pictures are presented on the right side. A simple discriminating strategy may be based on the grey value since bones, particularly their borders, tend to be lighter in colour than other structures.

Here we will provide a quick explanation of the processes that make up the MeVisLab network. A convolution filter is used to smoothen the picture and partly eliminate the noise that was previously created, after which some global and Otsu thresholding are performed. The second step is to use a linked components analysis. Given that bones are mostly connected structures, this enables the removal of a few tiny areas that were mistakenly detected before. The third step in picture smoothing is to apply a convolution filter once again. Lastly, the operator gives each of the six categories a unique label using a ROI selection tool. Specifically, the following anatomical groups have been selected: hips, sacrum, spine, ribs, sternum, and femoral bones (including the femoral head, neck, and upper portion of the femur). The clavicles and scapulae, which could only be seen in certain photos, are not shown here. It turns out that the spine and ribs are the most difficult groups to identify accurately. The former is because of their tiny and repetitive shape in a cross-sectional view, while the latter is mostly owing to the spinal canal, which is mistaken for bone. Right after the MeVisLab network semi-automated segmentation, a lot of

additional faults are discovered, therefore human labelling is necessary.

5.2 Manual data labeling

Manual inspection of individual scan slices follows the semi-automatic preprocessing. Observing a medical atlas rectifies the blunders. This is a tedious but necessary step before moving on to the next phase of the project. With MeVisLab's CSI tool, which lets you choose or deselect an area in a two-dimensional cross-sectional picture, much of the manual labelling is done. In particular, 3D views have been useful for identifying voxels that are noisy.

The most common errors made for each bone type during this procedure are summarized below:

Discs and bones. The spine's intricate design makes it one of the most difficult bone classes to identify. Incorrectly identifying the boundaries as ribs or filling the spinal canal with what seems to be bone are common problems with semi-automatic segmentation. Another crucial area that needs meticulous inspection are the slices that overlap with the sacrum.

The hips. At first, the hips are well segmented. The most common areas of error are the boundaries next to the femoral heads and, because to their fragility, some internal areas.

The back of the body. The areas seen in a cross-sectional picture of this long, flat bone is rather modest. Unfortunately, semi-automatic segmentation often misidentifies its limbs and the cartilage that joins it to the ribs.

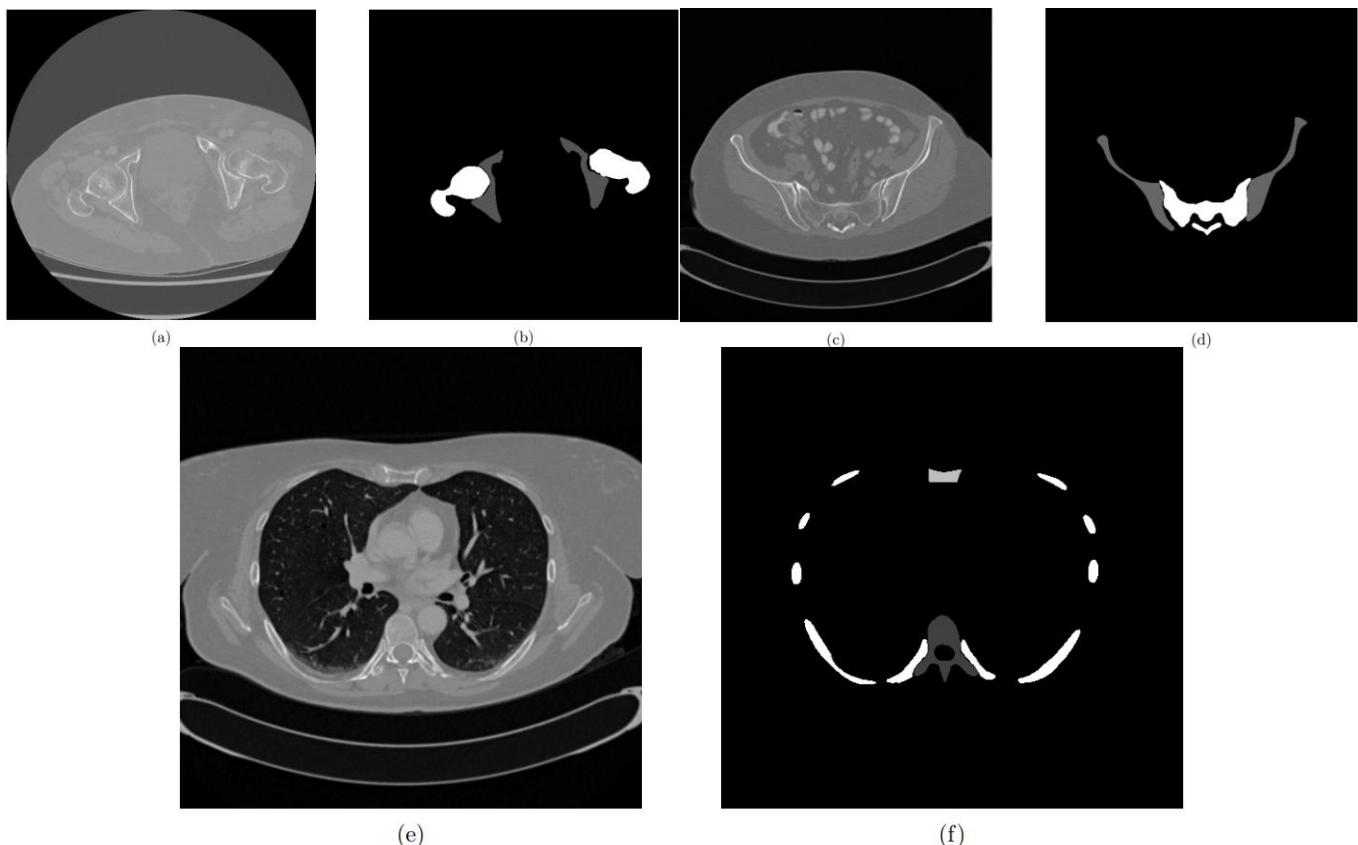


Fig 1: Training was conducted using three 2D pictures. The original photos are on the left side ((a), (c), (e)), while the bone masks are on the right side ((b), (d), (f)).

Ribs The cross-sectional form of this class makes it similarly difficult to segment. It has many discrete structures (f). Here, a three-dimensional picture is crucial for making sure that all of the split parts are really related in space. Another obstacle is avoiding the nearby cartilage.

Lower back. The sacrum is a challenging class to segment due to its complicated structure. The initial transverse slices show an overlap with the spine, starting from the top. In addition, the four sets of holes within the structure, called sacral foramina, are sometimes mistaken for bones.

Femoral bones. The most common cause of discolouration in femoral bones is that their interiors are somewhat darker than their exteriors. Thoroughly inspecting the junction with the hips is also necessary.

In addition, the clavicles and scapulae were also included of the first scans. The segmentation job did not take certain bones into account, thus they had to be manually deleted during post-processing. The three 2D original pictures and their corresponding masks. The masks in question were acquired subsequent to the manual data labelling procedure. A three-dimensional representation of a training labelled scan. For easier viewing, we've given each bone class a unique colour; however, when we labelled them, we gave them a greyscale value between 1 and 6, with 0 serving as the backdrop.

5.3 Data augmentation

Data augmentation involves applying changes in order to provide additional reliable training data for the primary training dataset. It is a regularization method that has been used effectively in many of the seminal articles published throughout the last several years within the field of deep learning. Typical transformations include translation (both horizontally and vertically), rotation, reflection, extraction of patches, changes in greyscale or colour values, and elastic deformations. Prior work on medical picture segmentation heavily relied on data augmentation to improve generalization from few annotated samples.

Due to the small quantity of tagged scans, data augmentation was necessary for this project. Indeed, overfitting occurs and validation dataset accuracy drops when only the original training dataset is used. Horizontal and vertical translation, rotation, magnification, and reflection are the random transformations employed. This means that between zero and five percent of the picture sizes are vertically and horizontally altered at random. After that, it's randomly scaled up to 95% of its horizontal size and 90% of its vertical size, and thereafter bent at an angle ranging from zero to five degrees. In the end, we produce a random integer between 0 and 1, and if it's more than 0.5, the picture is mirrored vertically. This was accomplished by modifying the Image Data Generator function of Keras so that the sample and mask would undergo the same modification at the same time. Using real-time data augmentation, the Keras function creates tensor image data in batches. The network implementation uses the central processing unit to supplement the data, with the graphics processing unit (GPU) training on batches of previously created data. Disc storage is limited to no more than 10 transformation batches at any one time. Because of this, the computational cost of data augmentation is minimal, and training time is not much increased. In addition, the network

sees new data every epoch due to the randomly applied modifications, which helps to minimize performance gap between training and validation/testing datasets.

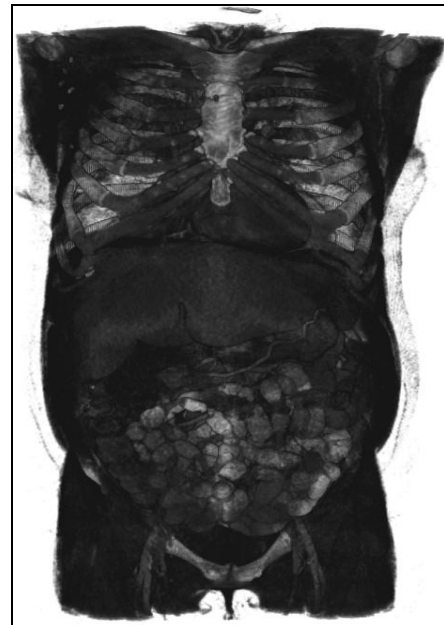


Fig 2: A three-dimensional representation of a CT scan of the abdomen.

6. Conclusion

Adding 3D convolutional layers to the network is a promising direction for future advancements. The network would have a better chance of achieving better segmentation accuracy and extracting more characteristics from the bones since they are three-dimensional structures. Particularly anticipated is improved segmentation of the ribs, which seem quite fractured in cross-sectional sections. Still, additional GPU memory and perhaps more training time would be necessary for this. Furthermore, an adversarial segmentation framework might be used to achieve additional advancements. Recent research has shown that adversarial training may enhance the segmentation masks produced throughout the course of a single CNN. To that end, our study suggests that training a CNN alongside an adversarial network might lead to better segmentation results.

Finally, our study proves that employing a CNN for autonomous bone segmentation and CT image categorisation is feasible. It turns out that the model is quite resistant to gaussian noise and has a high Dice coefficient. Having said that, we have noticed a number of limits and improvements that would undoubtedly boost performance. Various clinical and scientific applications in various medical activities might benefit from an enhanced but comparable model.

7. References

1. Yeshua T, Ladyzhensky S, Abu-Nasser A, *et al.* Deep learning for detection and 3D segmentation of maxillofacial bone lesions in conebeam CT. *Eur Radiol.* 2023;33:7507–7518. <https://doi.org/10.1007/s00330-023-09726-6>
2. Georgeanu VA, Mămuleanu M, Ghica S, Selișteanu D.

- Malignant bone tumors diagnosis using magnetic resonance imaging based on deep learning algorithms. *Medicina* (Kaunas). 2022;58(5):636. <https://doi.org/10.3390/medicina58050636>
3. Xu Z, Niu K, Tang S, Song T, Rong Y, Guo W, *et al.* Bone tumor necrosis rate detection in few-shot X-rays based on deep learning. *Comput Med Imaging Graph.* 2022;102:102141. <https://doi.org/10.1016/j.compmedimag.2022.102141>
 4. Tao Y, Huang X, Tan Y, Wang H, Jiang W, Chen Y, *et al.* Qualitative histopathological classification of primary bone tumors using deep learning: A pilot study. *Front Oncol.* 2021;11:735739. <https://doi.org/10.3389/fonc.2021.735739>
 5. Masoudi S, Mehralivand S, Harmon SA, *et al.* Deep learning based staging of bone lesions from computed tomography scans. *IEEE Access.* 2021;9:87531–87542. <https://doi.org/10.1109/ACCESS.2021.3074051>
 6. Alabdulkreem E, Saeed MK, Alotaibi SS, Allafi R, Mohamed A, Hamza MA. Bone cancer detection and classification using Owl Search Algorithm with deep learning on X-ray images. 2023.
 7. Yuvaraju M, Haripriya R. Calculation of bone disease using image processing. In: *Int Conf New Horizons Sci Eng Technol.* 2018.
 8. Avunuri P, Siramsetti P. Efficient ways to detect bone cancer using image segmentation process. *Int J Pure Appl Math.* 2018;118(14):1585–1592.
 9. Bourouis S, Chennoufi I, Hamrouni K. Multimodal bone cancer detection using fuzzy classification and variational model. In: *CIARP 2013, Part I, LNCS 8258.* Springer; c2013. p. 174–81.
 10. Anand D, Arulselvi G, Balaji G, Chandra GR. A deep convolutional extreme machine learning classification method to detect bone cancer from histopathological images. *Int J Intell Syst Appl Eng.* 2022;10(4):39–47. <https://ijisae.org/index.php/IJISAE/article/view/2194>
 11. Song L, Li C, Tan L, *et al.* A deep learning model to enhance the classification of primary bone tumors based on incomplete multimodal images in X-ray, CT, and MRI. *Cancer Imaging.* 2024;24:135. <https://doi.org/10.1186/s40644-024-00784-7>
 12. Sinthia P, Sujatha K. A novel approach to detect bone cancer using k-means clustering algorithm and edge detection method. 2016.
 13. Krizhevsky A, Sutskever I, Hinton GE. ImageNet classification with deep convolutional neural networks. *Adv Neural Inf Process Syst.* 2012;25:1097–105.
 14. Ronneberger O, Fischer P, Brox T. U-Net: Convolutional networks for biomedical image segmentation. In: *Med Image Comput Comput Assist Interv.* Springer; c2015. p. 234–41.

Creative Commons (CC) License

This article is an open access article distributed under the terms and conditions of the Creative Commons Attribution (CC BY 4.0) license. This license permits unrestricted use, distribution, and reproduction in any medium, provided the original author and source are credited.